Solving the Puzzle of ⟨100⟩ Interstitial Loop Formation in bcc Iron

Haixuan Xu (□□□), Roger E. Stoller, Yury N. Osetsky, and Dmitry Terentyev

Phys. Rev. Lett. **110**, 265503 — Published 26 June 2013

DOI: 10.1103/PhysRevLett.110.265503

Solving the Puzzle of <100> Interstitial Loop Formation in bcc Iron

Haixuan Xu (徐海謜) [1*], Roger. E. Stoller[1], Yury N. Osetskiy[1], and Dmitry Terentyev[2]

[1] Materials Science and Technology Division, Oak Ridge National Laboratory, Oak Ridge, TN 37831-6138, USA

[2] SCK-CEN, Nuclear Materials Science Institute, Boeretang 200, B-2400 Mol, Belgium

*E-mail: xuh1@ornl.gov

The interstitial loop is a unique signature of radiation damage in structural materials for nuclear and other advanced energy systems. Unlike other bcc metals, two types of interstitial loops, ½ <111> and <100>, are formed in bcc iron and its alloys. However, the mechanism by which <100> interstitial dislocation loops are formed has remained undetermined since they were first observed more than fifty years ago. We describe our atomistic simulations that have provided the first direct observation of <100> loop formation. The process was initially observed using our self-evolving atomistic kinetic Monte Carlo (SEAKMC) method, and subsequently confirmed using molecular dynamics simulations. Formation of <100> loops involves a distinctly atomistic interaction between two ½ <111> loops, and does not follow the conventional assumption of dislocation theory, which is Burgers vector conservation between the reactants and the product. The process observed is different from all previously proposed mechanisms. Thus, our observations might provide a direct link between experiments and simulations and new insights into defect formation that may provide a basis to increase the radiation resistance of these strategic materials.

Self-interstitial atoms are only found in materials far from equilibrium because of their high formation energies (~4eV). Therefore, interstitial loops are a principal signature of radiation damage created by neutrons or ions and are central to radiation-induced property changes in iron-based structural materials applied in current and advanced nuclear energy systems [1-6]. Large numbers of interstitial loops having both ½<111> and <100> Burgers vectors have been identified in bcc iron and its alloys. In contrast, almost exclusively ½<111> loops are observed in other bcc metals such as molybdenum, tungsten, and vanadium [7-9]. It has been proposed that the difference in irradiation response between iron and other bcc metals is related to the formation of these <100> loops [10]. In recent years molecular dynamics (MD) simulations in iron have demonstrated that small ½<111> interstitial clusters (nascent dislocation loops) are commonly formed directly in atomic displacement cascades, while the analog <100> clusters are rarely observed [11]. Since these two types of interstitial loops exhibit significantly different geometry and mobility at small sizes, they both contribute uniquely to microstructural evolution and the related mechanical properties. For instance, ½<111> loops have a migration energy less than 0.1 eV and may easily migrate to, and be absorbed by, other defects such as grain boundaries. As such, they would not be expected to accumulate to high densities. In contrast, the <100> loop is almost immobile and would accumulate in the microstructure if formed, acting as a stationary sink for mobile point defects. Therefore, unveiling the mysterious mechanism of <100> loop formation is of great importance for understanding radiation damage accumulation in iron and ultimately in predicting the properties of steels under extreme conditions.

In 1965, Eyre and Bullough proposed a mechanism which assumed that the nucleus of an interstitial loop consisted of interstitial atoms on a (110) plane in a configuration corresponding

to a faulted dislocation loop. They assumed that the stacking fault could be removed by shear involving either of the two following dislocation reactions [6]:

$$\frac{1}{2}[110]+\frac{1}{2}[001]=\frac{1}{2}[111] \quad (1a)$$

$$\frac{1}{2}[110]+\frac{1}{2}[\bar{1}10]=[010] \quad (1b)$$

However, it was subsequently realized that the high stacking fault energy in bcc iron makes the formation of faulted loops implausible; this was later confirmed by rigorous *ab initio* calculations [12]. Masters hypothesized that two ½<111> loops could interact and form a <100> loop although his study did not provide any experimental evidence [5]. According to dislocation theory, a simple Burgers vector sum of the appropriate ½<111> reactant loops can lead to a <001> loop as illustrated by the following example from Ref. 5:

$$\frac{1}{2}[111]+\frac{1}{2}[\bar{1}\bar{1}1]=[001] \quad (2)$$

During the past two decades, computer simulation has become a predominant tool for studying atomistic processes and several attempts have been made to discover the <100> loop formation mechanism [13-17]. For instance, Marian *et al.* proposed a modified version of the Eyre-Bullough mechanism based on the interactions they observed in MD simulations [14]. However, the complete process of <100> loop formation was not observed in MD simulations [13-15] or corroborated by any experimental evidence. Dudarev *et al.* developed an analytical model including the temperature dependence of the elastic self-energies of dislocations in iron; they found that <100> loops become energetically more favorable for temperatures above ~400°C [16]. This provides a thermodynamic explanation for <100> loop stability if formed, but sheds

no light on the formation mechanism. Calder *et al.* carried out MD displacement cascade simulations of very heavy ion bombardment and observed some <100> loops in the cascade debris. However, the probability of direct <100> loop formation in cascades created by neutron irradiation was estimated to be extremely low [17]. A number of experimental studies have also investigated loop formation in iron and dilute iron alloys [18-25]. The results indicate both <100> and ½<111> loops are formed under ion and neutron irradiation with the relative fraction depending on the irradiation temperature, dose, and solute (particularly Cr) content. However, the mechanism of <100> loop formation has not been determined.

Here we report for the first time direct observation of <100> loop formation from the interaction of two ½<111> loops in simulations using our recently developed self-evolving atomistic kinetic Monte Carlo (SEAKMC) [26, 27]. SEAKMC was developed to simulate dynamic atomistic processes with a fidelity to the underlying physics that is comparable to MD but able to reach much longer times. SEAKMC consists of four major components: selection of active volumes in which defects exist, saddle point searching for possible reactions, kinetic Monte Carlo to select reactions and advance time, and atomic relaxation of defect configurations. The details of this technique have been described elsewhere; it has been validated and benchmarked using MD simulations [26, 27]. An atomic structure and the interatomic potential are the only required material inputs. Active volumes with radii of 6.0 and 7.5 lattice constants (a_o) have been employed in cubic simulation cells with edge lengths of $20a_o$, $27a_o$ and $40a_o$. Each of these systems is much larger than the defect size, which is ~1.5 nm for a 37 interstitial cluster, and varying the system size over this range confirms the results are independent of system size. Furthermore, the lattice constants were scaled in accordance with the thermal expansion at each temperature so that the stress in the simulation box is negligible. The dimer method was used for

saddle point searches, with 60, 120, or 240 searches in each active volume to evaluate the sensitivity of the results to the number of searches. A constant attempt frequency of $1.0x10^{12}$ s^{-1} was used in all simulations. For each case, tens of simulations were carried out to obtain the requisite statistical precision. We have demonstrated previously that the number of dimer searches required to determine all possible reactions may be too high to be computationally tractable in some situations [27]. This absence of some reactions may introduce an error into the physical time calculated for any one simulation. However, the fact that the same process has been observed repeatedly in a large body of simulations implies this potential timing error does not affect the mechanisms that we observed or the conclusions described in this Letter. In addition, MD simulations were carried using the same initial input structure as for SEAKMC for each case studied. Three different interatomic potentials: A97, A04, and M07 (discussed below), are employed with the microcanonical (NVE) ensembles at different temperatures. The Verlet algorithm was used to integrate Newton's equation of motion with a time step of 0.1 femtoseconds. Simulations were run up to a few nanoseconds and Wigner-Seitz cells were used to determine the location and structure of defects. Tens of simulations were performed to obtain a statistical precision similar that of the SEAKMC.

We investigated ½<111> loops intersecting at both acute and obtuse angles as described in the *Supplemental Material*. The results presented here focus on the acute angle reactions since they are representative of both cases. In addition, the barrier for loops to react at an obtuse angle increases with size and loop reorientation leads larger loops to a final acute angle of interaction. Fig. 1 shows snapshots at different stages of the process for the observed interaction of two ½<111> loops. Fig. 1a contains the initial configuration and the Burgers vectors of these two loops are ½[111] and ½[$\bar{1}\bar{1}$1]. Both loops contain 37 interstitials (IC-37), corresponding to a

diameter of ~1 nm. These loops are highly mobile [28] and Fig. 1b shows the configuration after the two clusters encounter one another and their interaction forms a sessile junction. The sessile configuration is crucial because this provides an extended time for the individual interstitials in the loops to interact and evolve the configuration. In the previous studies mentioned above, similar sessile configurations were observed but they did not further evolve to any significant extent on MD time scales at the temperatures studied [26]. SEAKMC addresses this timescale problem, and Fig. 1c shows a change in the configuration of the sessile junction observed on the microsecond time scale (~0.2 μs) at 600K using this approach. The statistical variation of this time is relatively large, around one order of magnitude. This may be partly because of the incompleteness of the saddle point catalog, and more importantly due to the complex nature of the process, which involves many different reaction paths. This time-temperature combination indicates that the energy barrier for this process is relatively high. From this point, the configuration continues to evolve, resulting in a critical configuration in which about one-half of the defect configuration has a [100] orientation and the other half has a [111] orientation as shown in Fig. 1d. With further evolution, the [100] fraction may grow (Fig. 1e) and form a complete [100] loop (Fig. 1f). The loop formed had a rectangular shape, with a few unincorporated interstitials near the boundary. Multiple simulations indicate that loops are formed on both (100) and (110) habit planes. Note that the Burgers vector of the resultant loop is [100], not [001] as predicted by the often-assumed dislocation reaction in Eqn. (2). In fact, the observed Burgers vector is perpendicular to the one that is predicted by dislocation theory. In addition, we did not observe the intermediate <110> loops proposed previously [14]. This indicates that the mechanism of loop formation is not a simple dislocation reaction but rather a

complex atomistic process that involves the coordinated motion and rearrangement of the individual interstitials in the intermediate defect structure.

Furthermore, multiple simulations (>100 runs) have demonstrated that an evolution process which begins from the same initial configuration can lead to a variety of different final configurations, indicating that the transformation of the sessile complex into the final loop configuration is stochastic in nature. For instance, even when the system reaches the critical configuration (Fig. 1d), four outcomes are possible as shown in Fig. 2. The final <100> loop described previously can have a Burgers vector of either [100] or [010], or the process can lead to the formation of a <111>-type loop with either a ½[111] or ½$[\bar{1}\bar{1}1]$ Burgers vector. The reaction pathway for [100] loop formation involves a defect structure with part of the configuration in a [100] orientation, while the pathway of forming the ½<111> loops may or may not involve this particular intermediate state (see reaction pathways B and C in Fig. 2). Correspondingly, the formation of a small region with a [100] orientation does not guarantee that a [100] loop will be obtained (see reaction pathways A and B in Fig. 2). The fact that distinctly different outcomes can be obtained from the interaction of the same pair of reactant interstitial loops further illustrates how the atomistic process manifests itself and how different the atomistic process is from the commonly assumed dislocation reactions.

The SEAKMC approach employs empirical interatomic potentials just as MD does. In this work, we have employed three different interatomic potentials to evaluate their impact on the results. The potential of Ackland and co-workers from 1997 (A97) has been broadly used in radiation damage simulations [29]. However, it is widely known that the interstitial properties predicted by A97 are substantially different from those obtained from *ab initio* calculations. A more recent potential from 2004 (A04) significantly improved the predictions for interstitial defects [30].

A04 was subsequently modified by researchers in France (M07) to improve agreement with a larger set of *ab initio* data on interstitial clusters, including the behavior of sessile clusters[31, 32]. A04 and M07 represent the state of art in describing bcc iron. Our SEAKMC simulations using A97 did not lead to the complete formation of a <100> loop. The results were consistent with those of Marian, *et al.*, in which a sessile junction was formed [14], but the transformation to a <100> loop was not completed. This is likely due the fact that interstitial defects are not properly described by this potential. Essentially the same mechanisms for <100> loop formation were found using either A04 or M07 for both the acute and obtuse reaction angles. Some detailed differences between these two potentials in the formation process will be reported elsewhere.

It appears that the previous attempts to observe <100> loop formation using MD simulations failed either due to the shortcomings of the potential that was employed [14], or because very high temperatures were used to compensate for the relatively short times accessible by MD [15]. With the guidance provided by our experience with SEAKMC, we carried out more than 200 MD simulations using the A97, A04, and M07 potentials at various temperatures. The <100> loop formation mechanism has been confirmed in MD simulations using M07 potentials; consistent with the SEAKMC results it was not observed using A97. An MD example for two IC-37s using M07 is shown in Supplementary Materials. Observation of the same process using these two different atomistic methods, and two different potentials, provides high confidence in the mechanism reported here.

The results of our simulations demonstrated that the stability of <100> and ½<111> loops was quite similar for the small to intermediate sized reactant loops (IC-19, IC-37, and IC-61) considered in this study. The relevant energy landscape for two IC-37s using M07 is shown in Fig. 3, where the final mean energy values for the A, B, and C configurations are similar. The

limiting energy barrier along the various reaction pathways is indistinguishable and is estimated to be 0.73 ± 0.11 eV. The similar stability of the alternative loop configurations is consistent with the experimental observation of fluctuations in Burgers vector of small loops under electron irradiation or simple heating [21]. The inset table in Fig.3 indicates the relative probability of the A, B, and C paths obtained in simulations including the three cluster sizes, multiple temperatures, and all three potentials. The simulations listed as incomplete involved primarily the largest size (IC-61) or the A97 potential.

In summary, the first observation of complete <100> loop formation from two interacting ½ <111> loops has been presented. The mechanism involves a detailed atomistic process with the reaction product having a Burgers vector that is not consistent with previously proposed mechanisms that assumed a sum of the reactant loops as in Eqn. (2). The interaction between interstitial loops is stochastic in nature and distinctly different outcomes can be obtained from the same initial configuration. The results of this research provide the answer to the long-standing question of how <100> loops are formed and will have a direct impact on our understanding of radiation damage evolution in iron-based alloys. In addition, this mechanism may also provide insights into other atomistic processes that are of interest to the materials physics community. This understanding, along with further research and development, may enable the control of loop evolution (and potentially the radiation resistance) of these materials. For example, the experimentally observed ratio of <100> to ½<111> dislocation loops depends on neutron fluence, irradiation temperature and alloy chemistry. In the case of commercially important Fe-Cr alloys, increasing the Cr concentration reduces the fraction of <100> loops observed after irradiation [18-20, 24, 25]. Addition of Cr also reduces the mobility of ½<111> loops [33]. Since the mobile ½<111> clusters are formed directly in displacement cascades, the change in the <100> loop

fraction may well be related to this effect of Cr. In the context of the <100> loop formation mechanism proposed here, the Cr interaction that leads to reduced ½<111> defect mobility may reduce the formation of <100> loops by increasing the fraction of loop-loop interactions that follow pathways B and C in Fig. 2. This possibility will be assessed in future simulations of Fe-Cr using our SEAKMC approach.

Acknowledgements

Research sponsored by the U.S. Department of Energy, Office of Basic Energy Sciences, Materials Sciences and Engineering Division, "Center for Defect Physics," an Energy Frontier Research Center. The authors would like to thank G.M. Stocks, D.J. Bacon, and A. Barashev for their valuable comments on the manuscript.

Reference

[1] B. Raj, and M. Vijayalakshmi, in *Comprehensive Nuclear Materials*, edited by R. J. M. Konings *et al.* (Elsevier Ltd., Amsterdam, 2012), pp. 97.

[2] R. L. Klueh, and D. R. Harries, *High-Chromium Ferritic and Martensitic Steels for Nuclear Applications* (American Society for Testing and Materials, West Conshohocken, PA, 2001), ASTM' Monograph Series, Monograph 3.

[3] B. L. Eyre, Philos. Mag. **7**, 2107 (1962).

[4] B. L. Eyre, and A. F. Bartlett, Philos. Mag. **12**, 261 (1965).

[5] B. C. Masters, Philos. Mag. **11**, 881 (1965).

[6] B. L. Eyre, and R. Bullough, Philos. Mag. **12**, 31 (1965).

[7] R. C. Rau, F. S. D'Aragona, and R. L. Ladd, Philos. Mag. **21**, 441 (1970).

[8] P. M. Rice, and S. J. Zinkle, J. Nucl. Mater. **258**, 1414 (1998).

[9] T. Matsui, S. Muto, and T. Tanabe, J. Nucl. Mater. **283**, 1139 (2000).

[10] E. A. Little, R. Bullough, and M. H. Wood, Proc. Roy. Soc. Lond. A **372**, 565 (1980).

[11] R. E. Stoller, in *Comprehensive Nuclear Materials*, edited by R. J. M. Konings *et al.* (Elsevier Ltd., Amsterdam, 2012), pp. 293.

[12] F. Willaime *et al.*, Nucl Instrum Meth B **228**, 92 (2005).

[13] Y. N. Osetsky, A. Serra, and V. Priego, J. Nucl. Mater. **276**, 202 (2000).

[14] J. Marian, B. D. Wirth, and J. M. Perlado, Phys. Rev. Lett. **88**, 255507 (2002).

[15] D. Terentyev *et al.*, J. Nucl. Mater. **382**, 126 (2008).

[16] S. L. Dudarev, R. Bullough, and P. M. Derlet, Phys. Rev. Lett. **100**, 135503 (2008).

[17] A. F. Calder *et al.*, Philos. Mag. **90**, 863 (2010).

[18] Z. Yao *et al.*, Philos. Mag. **88**, 2851 (2008).

[19] M. Hernandez-Mayoral *et al.*, Philos. Mag. **88**, 2881 (2008).

[20] M. L. Jenkins *et al.*, J. Nucl. Mater. **389**, 197 (2009).

[21] K. Arakawa *et al.*, Phys. Rev. Lett. **96**, 125506 (2006).

[22] K. Arakawa *et al.*, Science **318**, 956 (2007).

[23] K. Arakawa, T. Amino, and H. Mori, Acta Mater. **59**, 141 (2011).

[24] A. C. Nicol, M. L. Jenkins, and M. A. Kirk, in *MRS Fall Meeting* (MRS Proceedings, Boston, MA, 2000).

[25] L. L. Horton, J. Bentley, and K. Farrell, J. Nucl. Mater. **108**, 222 (1982).

[26] H. X. Xu, Y. N. Osetsky, and R. E. Stoller, Phys. Rev. B **84**, 132103 (2011).

[27] H. X. Xu, Y. N. Osetsky, and R. E. Stoller, J. Phys-Condens. Mat. **24**, 375402 (2012).

[28] N. Anento, A. Serra, and Y. N. Osetsky, Model. Simul. Mater. Sc. **18** (2010).

[29] G. J. Ackland *et al.*, Philos. Mag. A **75**, 713 (1997).

[30] G. J. Ackland *et al.*, J. Phys-Condens. Mat. **16**, S2629 (2004).

[31] L. Malerba *et al.*, J. Nucl. Mater. **406**, 19 (2010).

[32] M. C. Marinica, F. Willaime, and J. P. Crocombette, Phys. Rev. Lett. **108**, 025501 (2012).

[33] D. Terentyev, L. Malerba, and A. V. Barashev, Phil. Mag. Lett. **85**, 587 (2005).

Figure 1 Snapshots at different times during the transformation process using Wigner-Seitz analysis. Spheres are atoms and boxes are vacant lattice sites. The lines indicate the vector between each atom and the closest lattice site. The colors indicate the orientation of individual interstitial from blue (<111>) to red ([100])

Figure 2 Summary of the possible outcomes from two ½<111> loop interactions for acute angle after a sessile junction is formed. Reaction Paths A and B share the intermediate configuration that involves partial [100] orientation. Reaction Path C does not involve partial [100] orientation. The viewing direction is [100].

Figure 3 Typical changes in system energy as the defect configuration evolves for reaction of two IC-37 with Burgers vectors ½[111] and ½[$\bar{1}\bar{1}$1]; width of curves indicates the standard deviation of the energy values. The energy barriers associated with the different reaction paths are very similar and are estimated to 0.73 ± 0.11 eV. The probability of each reaction path from SEAKMC is shown in the inset table. The reference state is taken as the energy of the system with two well-separated loops.

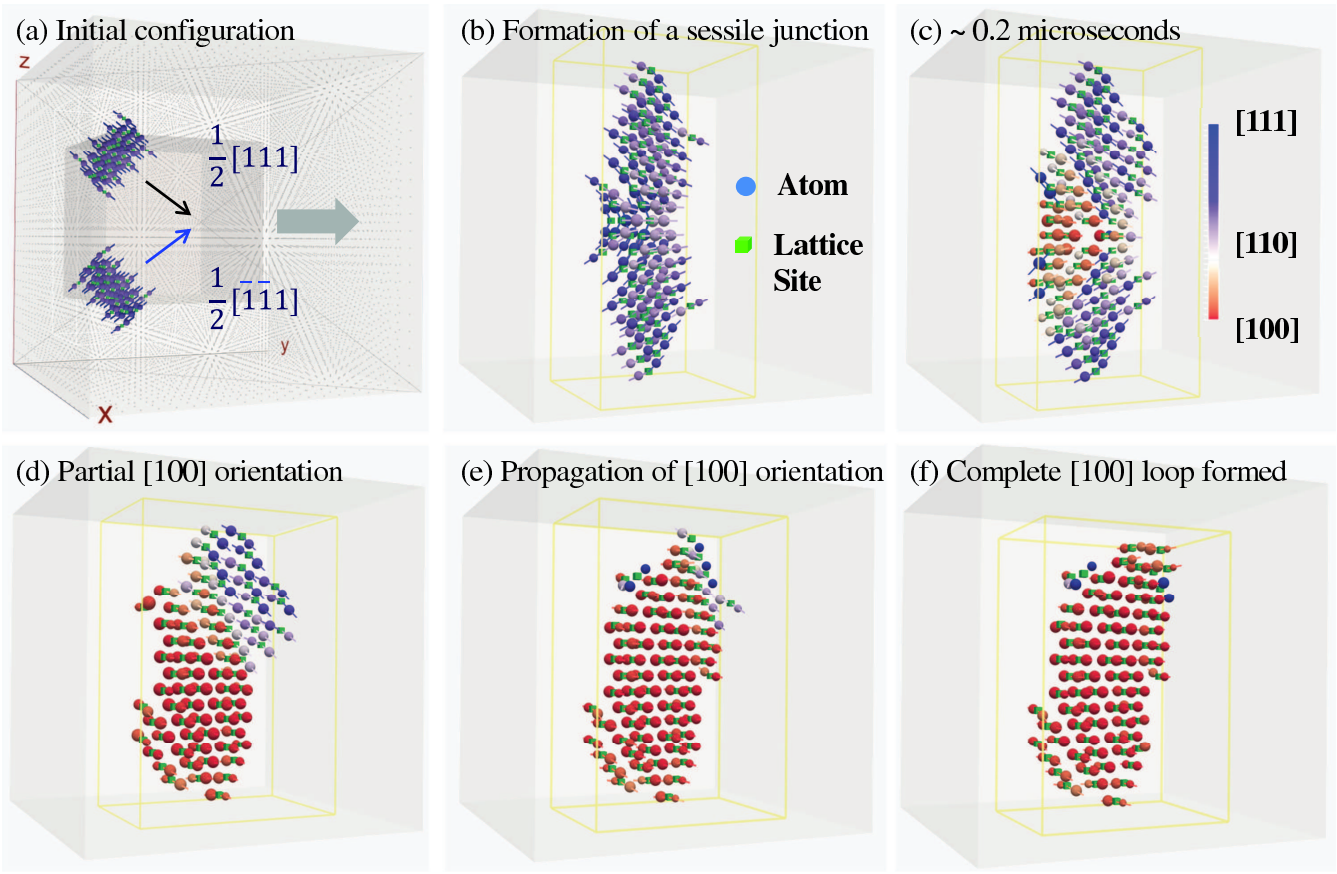

Figure 1 LB13954 30MAY2013

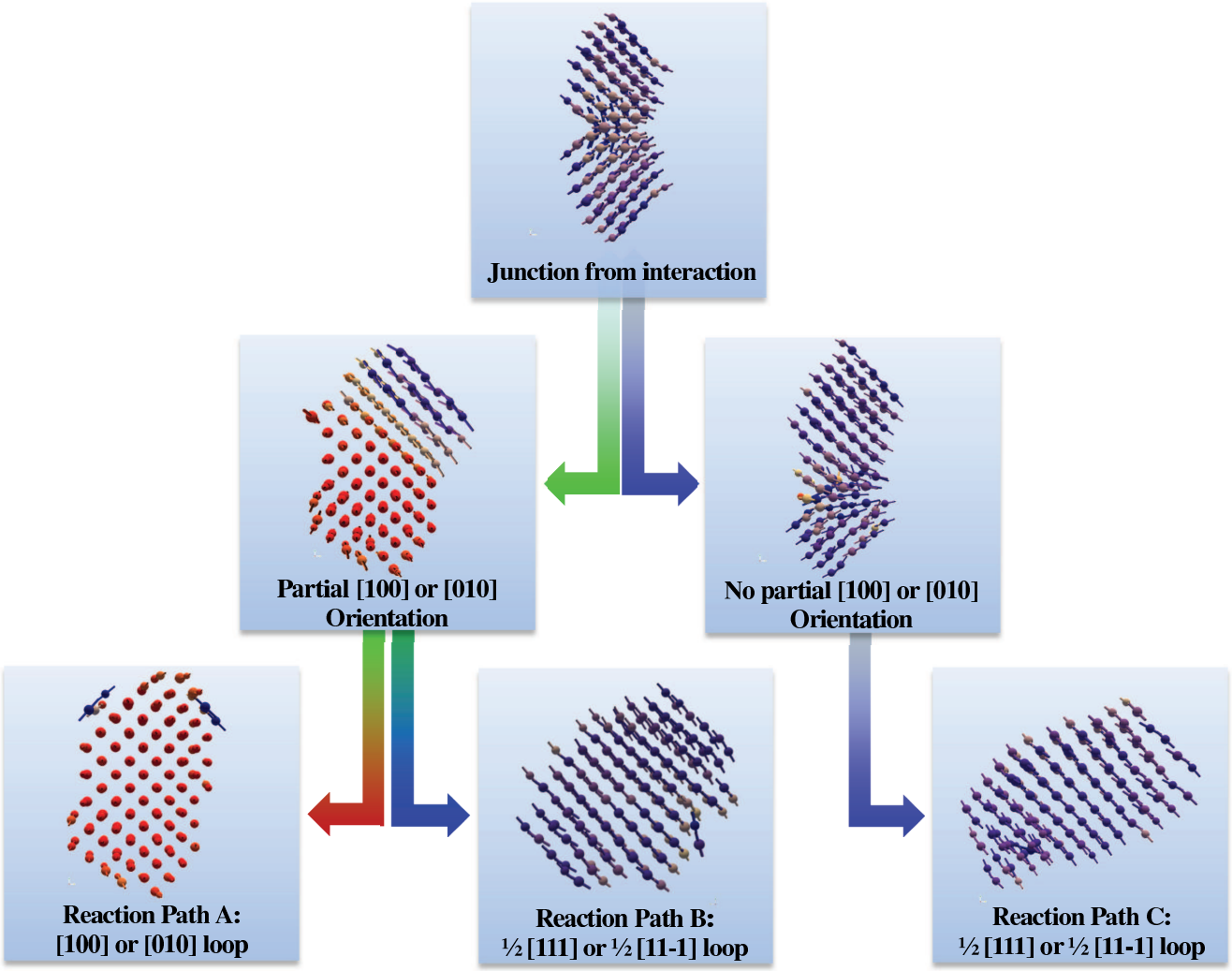

Figure 2 LB13954 30MAY2013

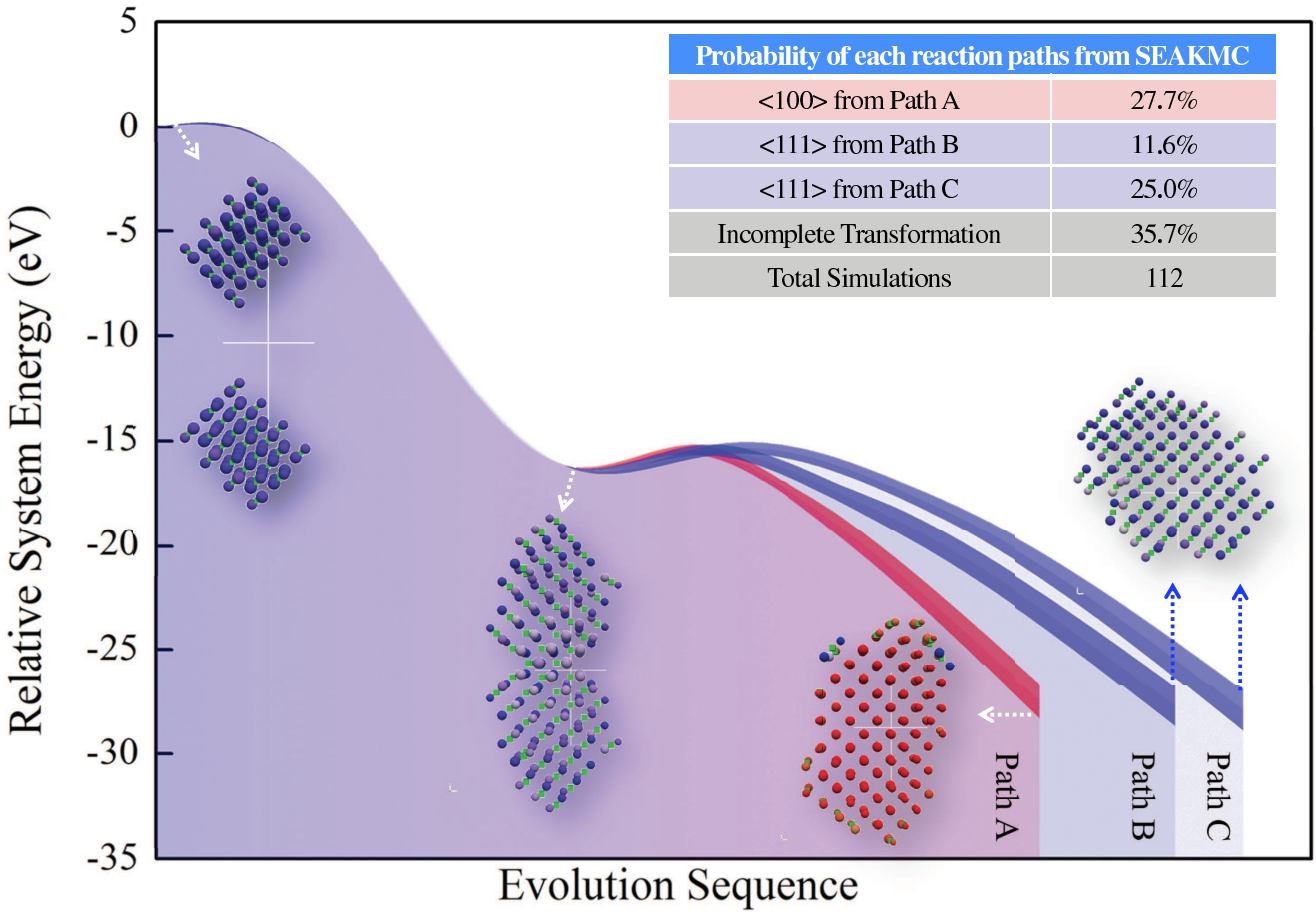

Figure 3 LB13954 30MAY2013